Title.

Aggregation-prone peptides modulate activity of bovine interferon gamma released from naturally occurring protein nanoparticles

Author names and affiliations.

José Vicente Carratalá[a,b], Olivia Cano-Garrido[a,b,c,1], Julieta Sánchez[a,2], Cristina Membrado[a,b], Eudald Pérez[a,b], Oscar Conchillo-Solé[a], Xavier Daura[a,d], Alejandro Sánchez-Chardi[e], Antonio Villaverde[a,b,c], Anna Arís[f], Elena Garcia-Fruitós[f], Neus Ferrer-Miralles[a,b,c]#

[a]Institut de Biotecnologia i de Biomedicina, Universitat Autònoma de Barcelona, Bellaterra, Barcelona, Spain

[b]Departament de Genètica i de Microbiologia, Universitat Autònoma de Barcelona, Bellaterra, Barcelona, Spain

[c]CIBER de Bioingeniería, Biomateriales y Nanomedicina (CIBER-BBN), Bellaterra, Barcelona, Spain

[d]Catalan Institution for Research and Advanced Studies, Barcelona, Spain

[e] Departament de Biologia Evolutiva, Ecologia i CiènciesAmbientals, Facultat de Biologia, Universitat de Barcelona, Av. Diagonal 643, 08028 Barcelona, Spain.

[f]Department of Ruminant Production, Institut de Recerca i Tecnologia Agroalimentàries (IRTA), Caldes de Montbui, Barcelona, Spain

#Address correspondence to Neus Ferrer-Miralles, neus.ferrer@uab.cat.

[1]Present address: Nanoligent SL. Edifici Eureka. Av. de Can Domènech s/n. Campus de la UAB. Bellaterra, Barcelona, Spain

[2]Permanent address: Universidad Nacional de Córdoba, Facultad de Ciencias Exactas, Físicas y Naturales, ICTA and Departamento de Química, Cátedra de Química Biológica, Córdoba, Argentina, CONICET, Instituto de Investigaciones Biológicas y Tecnológicas (IIBYT), Córdoba, Argentina.

Abstract

Efficient protocols for the production of recombinant proteins are indispensable for the development of the biopharmaceutical sector. Accumulation of recombinant proteins in naturally-occurring protein aggregates is detrimental to biopharmaceutical development. In recent years, the view of protein aggregates has completely changed with the recognition that these aggregates are a valuable source of functional recombinant proteins. In this study, bovine interferon-gamma (rBoIFN-γ) was engineered to enhance the formation of protein aggregates (also known as protein nanoparticles (NPs)) by the addition of aggregation-prone peptides (APPs) in the generally recognized as safe (GRAS) bacterial *Lactococcus lactis* expression system. The L6K2, HALRU and CYOB peptides were

selected to assess their intrinsic aggregation capability to nucleate protein aggregation. These APPs enhanced the tendency to aggregate of the resulting protein at the expense of the total protein yield. However, fine physico-chemical characterization of the resulting intracellular protein NPs, the protein released from these protein NPs, and the protein purified from the soluble cell fraction indicated that the compactability of protein conformations is directly related to the biological activity of variants of IFN-γ, which is used here as a model protein with therapeutic potential. APPs enhance aggregation tendency of fused rBoIFN-γ while increasing compactability of protein species. Biological activity rBoIFN-γ is favored in more compacted conformations. Naturally-occurring protein aggregates can be produced in GRAS microorganisms as protein depots of releasable active protein. The addition of APPs to enhance aggregation tendency has a positive impact in overall compactability and functionality of resulting protein conformers.

Keywords

Interferon-gamma, protein nanoparticles, protein aggregation, *Lactococcus lactis*, GRAS, conformational compactability

1. Introduction

59 The efficient production and purification of recombinant proteins in a wide range of
60 expression hosts has driven the launch of a large number of biopharmaceutical products.
61 One of the most-studied expression systems is *Escherichia coli* (*E. coli*), which is also one of
62 the most-used gene expression systems for biopharmaceutical products [1,2]. However,
63 pro-inflammatory contaminant lipopolysaccharide (LPS) components of the outer leaflet
64 of the outer membrane of *E. coli* need to be removed from the purified protein to ensure
65 the safety of the final product, increasing the final cost [3,4]. Prokaryotic endotoxin-free
66 expression systems are being explored to overcome this limitation, including *E. coli* LPS
67 mutant strains [5,6] and generally recognized as safe (GRAS) microorganisms, such as
68 *Lactococcus lactis* (*L. lactis*) [7,8]. These strains are envisioned as sound alternatives that
69 avoid the safety concern of LPS contamination retaining the advantages of culturing
70 prokaryotic hosts [9,10].

71 During recombinant gene expression, the great stress posed to the protein quality control
72 machinery leads, in most cases, to the accumulation of the recombinant protein in
73 aggregates that form intracellular nanoparticles (NPs), known as inclusion bodies (IBs) [11-
74 13]. In fact, the aggregation of a heterologous is one of the evaluated key parameters
75 when stablishing the production and purification processes [14-16]. Intracellular protein
76 aggregates are dynamic and complex nanostructures with a variable content of
77 recombinant protein [17-19]. The trapped protein was formerly thought to be biologically
78 inert due to, aberrant protein conformations or inactive partially folded species
79 incompatible with the presence of biological activity. Thus, the recombinant protein could
80 be often recovered, with low efficiency, from the insoluble cell fraction by *in vitro*

81 denaturing/refolding processes [20]. This scenario has been replicated in biotechnological
82 research, and the main goal of recombinant protein production is to minimize protein
83 aggregation (and, in consequence, maximize protein solubility) during the production
84 process.

85 However, in recent decades, the view of naturally occurring protein aggregates as inert
86 material has changed completely since the detection of biologically active protein
87 embedded in these aggregates [21-23]. The classic view of protein aggregates as mere
88 inactive folding intermediates has been transformed into the idea of heterogeneous
89 porous multimeric structures stabilized by a scaffold of cross beta-sheet structures that
90 contain conformers of the recombinant protein in which a spectrum of recombinant
91 protein species containing native-like conformations are incorporated [12]. In fact, it has
92 been proven that biologically active protein species can be extracted from IBs by applying
93 mild solubilization protocols, indicating the biologically active nature of proteins forming
94 these aggregates [24]. In addition, further ground-breaking studies have suggested
95 applications of IBs in nanomedicine. In these studies, IBs are envisioned as recombinant
96 protein depots capable of slow release of active recombinant protein to replace specific
97 biological activities in defective cell lines, to recover cell viability under stress conditions in
98 cell culture [25], or even to target specific cell types in tumors when subcutaneously
99 implanted in animal models [26,27]. Furthermore, IBs have been proposed as a novel
100 biomaterial for use in tissue engineering due to the stimulation of mechanical and physical
101 signals induced in surrounding cells, even in the absence of cell growth-promoting protein
102 factors in their formulation [28,29]. Therefore, IBs are envisioned as non-toxic,

103 biocompatible and mechanically stable materials from which biologically active molecules
104 of the recombinant protein can be released under mild solubilization and physiological
105 conditions.

106 In this scenario, interest in the possibility of controlling the aggregation of recombinant
107 proteins in these types of nanostructures is increasing, and several aggregation-prone
108 peptides (APPs) have been identified for fusion with recombinant proteins to enhance the
109 aggregation process in the producing cell [30]. In this study, we selected interferon-
110 gamma (IFN-γ) as a model protein to study the effect of the addition of APPs in naturally
111 occurring protein aggregates due to interest in this activity in biomedicine and its
112 potential use in animal health.

113 IFN-γ is the sole type II IFN. This cytokine is produced and secreted by different cell types
114 and is involved in immunostimulatory processes through the activation of specific cellular
115 pathways at the transcriptional level [31]. IFN-γ secretion, by natural killer (NK) cells and
116 antigen-presenting cells (APCs), enhances the innate immune response against detected
117 pathogens, while T-lymphocytes are involved in the secretion of IFN-γ in the adaptive
118 immune response [32,33]. IFN-γ secretion is mainly regulated by other cytokines produced
119 by APCs, including IL-12 and IL-18. The activity of IFN-γ depends on its interaction, as a
120 dimer, with the IFN-γ receptor (IFNGR). IFNGR is a tetrameric complex formed by two
121 ligand-binding proteins (IFNGR1) and two signal-transducing proteins (IFNGR2).

122 IFN-γ is one of the biopharmaceuticals approved by the FDA under the trade name
123 ACTIMMUNE® (Horizon Pharma, Inc., USA). An Iranian biosimilar (γ-IMMUNEX, Exir

Pharmaceutical Company, Iran) is distributed in Asia. IFN-γ is used to prevent infectious diseases in patients suffering from chronic granulomatous disease and is also indicated to slow osteopetrosis [34]. In recent years, IFN-γ has been investigated in approximately 80 clinical trials for a number of indications, mainly related to immune system disorders, infectious diseases and cancer (https://www.clinicaltrials.gov). Recombinant IFN-γ is administered either as a unique drug in these clinical trials [35-41] or in combination with other products [42-44]. Therefore, the central key role of IFN-γ in immunostimulatory and immunomodulatory effects will lead to an increase in the use of this cytokine in the coming years in human health. The immunostimulatory properties of this cytokine have also been evaluated as alternative therapeutics in animal health [45]. In fact, the administration of IFN-γ by intramammary infusion in productive dairy cows for mastitis treatment has been proposed as a putative strategy to reduce the spread of antibiotic resistance among zoonotic bacteria [46]. Furthermore, the wide use of antibiotics in the prevention of animal diseases and growth promotion appears to be a source of resistant bacteria, and WHO and the United Nations have deployed global action against this threat to health security. Therefore, the rational use of antibiotics in addition to the development of immunostimulatory alternatives in the treatment and prevention of animal diseases may play a role in the control of antibiotic resistance.

Interestingly, recombinant products for animal health must not only be stable and safely and effectively delivered on a large scale and under standard conditions but also present obvious advantages over existing products to prove its commercial viability [47]. In this context, approved recombinant human IFN-γ can be obtained from the *E. coli*

146 expression system, but novel protein formulations need to be developed. In fact, in most
147 reported studies of the expression and purification of IFN-γ, the recombinant protein is
148 recovered from the purified IBs through extensive denaturation-refolding processes [48-
149 50].

150 Given the importance of expanding the catalogue of prokaryotic expression strains to
151 improve biophamaceutical safety, to explore the possibility of formulating recombinant
152 proteins in alternative cost-effective formats and developing novel treatments to reduce
153 the reliance on antibiotics, in this work, we produced recombinant bovine IFN-γ (rBoIFN-γ)
154 in GRAS lactic acid bacteria (*L. lactis*) in the form of protein NPs. We analyzed the ability of
155 APPs fused to rBoIFN-γ to enhance the aggregation propensity of the recombinant
156 cytokine. Furthermore, we assessed the link between the biological activities contained in
157 protein NPs of IFN-γ variants and their physico-chemical characteristics. We determined
158 that the activity of the IBs is related to the specific biological activity of the recombinant
159 protein they contain, whereas the proportion of released protein is not the main factor.
160 The data presented here illustrate the great potential of endotoxin-free protein NPs as
161 active biomaterials to formulate, at the nanoscale level, releasable proteins of biomedical
162 interest.

163 **2. Materials and methods**

164 **2.1. Bacterial strains and plasmids**

165 *E. coli* MC4100 (StrepR) [51] was used for cloning genes for protein production in *L.*
166 *lactis*. *E. coli* DH5α was used for cloning genes for protein production in *E. coli*. *L. lactis*

cremoris NZ9000 (Boca Scientific), and *ClearColi®* BL21(DE3) (Lucigen) were used in expression experiments for each expression system. For *L. lactis* expression vectors, IFN-γ of bovine (*Bos taurus*) origin was cloned at the *Nco*I/*Xba*I restriction sites of the CmR pNZ8148 plasmid (MoBiTech). The digestion products were ligated into the expression plasmid pNZ8148, and ligation product was used to transform *L. lactis* NZ9000 competent cells by electroporation [52]. Electroporation was performed using a Gene Pulser from Bio-Rad with settings of 2500 V, 200 Ω and 25 µF in a pre-cooled 2-cm electroporation cuvette. The electroporated cells were then supplemented with 900 µl of M17 broth with 0.5 % glucose and incubated for 2 h at 30 °C. The electroporation mix was centrifuged for 10 min at 10,000 x *g* at 4 °C, and the pellet was resuspended in 100–200 µl of M17 media and plated. In addition, fusions of rBpIFN-γ with APPs were constructed (rBOIFN-γ_L6K2, rBoIFN-γ_HALRU and rBoIFN-γ_CYOB). All genes were C-terminally fused to a His-tag for detection and quantification by western blot analysis. A Lys residue was included at the N-terminus of the tag for putative elimination of the tag by exopeptidases. Gene sequences were codon optimized for the *L. lactis* expression host as indicated (Geneart). For the *E. coli* expression vector pETDuet (Novagen), the *L. lactis* codon-optimized IFN-γ gene of bovine (*Bos taurus*) origin was cloned at the *Nco*I/*Hin*dIII restriction sites of the pETDuet plasmid. The expression vector was transformed into the *ClearColi®* BL21(DE3) strain. Electroporation was performed using a Gene Pulser from Bio-Rad with settings at 2400 V, 750 Ω and 25 µF in a pre-cooled 2-cm electroporation cuvette. The electroporated cells were then supplemented with 900 µl of lysogeny broth (LB) and incubated for 1 h at 37 °C. The cells were then plated on LB-agar plates containing ampicillin (100 µg/ml) and

189 incubated at 37 °C overnight. For all clones, in the sequence design we added an *Nco*I
190 restriction site at the 5′ end followed by the nucleotides CA to restore the reading frame.
191 This cloning strategy adds an Ala to the N-terminus of the protein. Therefore, the
192 recombinant proteins were produced as the mature form of the IFN-γ (from Gln24 to
193 Thr166 NP_776511.1) with an additional Ala at the N-terminus to restore the frameshift
194 introduced by the *Nco*I restriction site (Fig. 1a).

195 **2.2. Selection of aggregation-prone peptides (APPs)**

196 APPs were selected by scanning the Disprot v6.02 database [53] with AGGRESCAN
197 software [54]. We selected two unstructured regions from two different proteins that
198 displayed a higher HSA. This selection was based on the assumption that APPs in solvent-
199 exposed regions were the best candidates for the purposes of this study. Additionally,
200 L6K2 was selected based on previous experimental results [55] after analysis with
201 AGGRESCAN showed that this peptide had a high NHSA and high a^4vAHS.

202

203 **2.3. Production and purification of rBoIFN-γ protein from the soluble cell fraction**

204 Cultures of *ClearColi®* BL21 (DE3) cells transformed with the plasmid containing rBoIFN-
205 γ gene (pETDuet-rBoIFN-γ) were incubated in a shake flask at 37 °C and 250 rpm in LB
206 medium supplemented with 100 μg/ml ampicillin. When the cultures reached an
207 OD 550 of approximately 0.5 – 0.7, protein expression was induced by adding 1 mM IPTG
208 (isopropyl-β-D-thiogalactopyranoside). The cultures were then incubated at 20 °C and
209 250 rpm overnight (for protein production). During the purification process, cells were

collected by centrifugation (15 min, 6,000 x *g*, 4 °C), and proteins were released by sonication. Briefly, cells were lysed by sonication with 5 rounds of 3-min cycles and pulses of 0.5 s at 15 % amplitude (Lab Sonic ultrasonicator). *L. lactis cremoris* cells transformed with plasmids containing the rBoIFN-γ gene (pNZ8148-rBoIFN-γ, pNZ8148-rBoIFN-γ_L6K2, pNZ8148-rBoIFN-γ_HALRU and pNZ8148-rBoIFN-γ_CYOB) were incubated in a shake flask at 30 °C without shaking in M17 broth + 0.5 % glucose supplemented with 5 μg/ml chloramphenicol and 2.5 μg/ml erythromycin. When the cultures reached an OD 550 of approximately 0.4-0.6, protein expression was induced by adding 12.5 ng/ml nisin. Then, the cultures were incubated at 30 °C without shaking for the indicated time. The cells were collected by centrifugation (15 min, 6,000 x *g*, 4 °C), and proteins were released by a French press (3 rounds at 15000 PSI/machine pressure).

From this point, the same protocol was followed for both proteins. The soluble and insoluble cell fractions were separated by centrifugation (40 min, 15,000 x *g*, 4 °C), and the soluble cell fraction was filtered using a pore diameter of 0.2 μm. The recombinant protein in the soluble cell fraction was purified by immobilized metal affinity chromatography (IMAC) using a HiTrap Chelating HP 1-ml column (GE Healthcare) with an ÄKTA purifier FPLC system (GE Healthcare). The eluted proteins were then dialyzed against phosphate-buffered saline (PBS) buffer. The control protein rBoIFN-γ_Std (produced in *E. coli*) was obtained from R&D Systems (2300-BG-025, R&D Systems) and corresponded to a mixture of bovine IFN-γ Gln24-Thr166 and Gln24-Arg162, both with an N-terminal.

231 **2.4. Production and purification of rBoIFN-γ protein nanoparticles.**

232 *L. lactis* cells transformed with expression plasmids derived from pNZ8148 were grown
233 in M17 medium enriched with 0.5 % glucose at 30 °C without shaking. *E. coli* was grown in
234 LB rich medium at 37 °C and 250 rpm. NP production was induced by adding 12.5 ng/ml
235 nisin (Sigma-Aldrich) to *L. lactis* or 1 mM IPTG to *E. coli* cultures. After induction, the
236 cultures were grown for 5 h. Antibiotics were used for plasmid maintenance at the
237 following concentrations: chloramphenicol (5 μg/ml) and erythromycin (2.5 μg/ml) for *L.*
238 *lactis* and ampicillin (100 μg/ml) and streptomycin (30 μg/ml) for *ClearColi*.

239 Once produced, the protein NPs were purified using the purification protocol described
240 previously [9], including, at the beginning of the process, a mechanical disruption step by
241 French press. The protocol was performed under sterile conditions and all incubations
242 were carried out under agitation. The purified protein NPs were diluted 1:10 in PBS and
243 resuspended.

244

245 **2.5. Quantitative protein analysis**

246 The amounts of recombinant proteins produced by the expressing cells or present in
247 NPs were quantified by denaturing SDS-PAGE as described previously [56]. Bands were
248 identified using a commercial polyclonal serum against the histidine tag (#A00186-100
249 Genscript) and an anti-mouse secondary antibody (#170-6516, Bio-Rad). The recombinant
250 protein yield was estimated by comparison with a standard curve of known amounts of a

purified GFP-H6 protein quantified by the Bradford assay. Quantification was performed with Quantity One software (Bio-Rad).

2.6. Ultrastructural characterization

To characterize the morphometry (size and shape) of the NPs, microdrops of protein aggregate suspensions were deposited for 2 min on silicon wafers (Ted Pella Inc.), air-dried and observed in a nearly native state under a field emission scanning electron microscope (FESEM) Zeiss Merlin (Zeiss) operating at 1 kV. Micrographs of the NPs were acquired with a high-resolution in-lens secondary electron (SE) detector. Images were taken at magnifications ranging from 20,000x to 80,000x.

2.7. Z potential analysis

Z potential (ZP) characterization of each kind of protein NPs was carried out using DLS equipment (Malvern Nanosizer). To prevent the electrodes from burning, the samples were prepared in deionized (MilliQ) water, a low ionic strength medium. Each sample was analyzed in triplicate.

2.8. Determination of rBoIFN-γ biological activity in bovine cells

The different rBoIFN-γ formulations described here were analyzed by a modified kynurenine bioassay [57]. Bovine fibroblast-like cells (EBTr cells), (87090202 Sigma-Aldrich) were cultured in Dulbecco's modified Eagle's medium (Gibco) with 10 % fetal bovine serum (FBS). Depending on cell growth, cultures were split every 2 days using

ratios of 1:2 to 1:3. Before an experiment, a lower ratio was selected to obtain the maximum cell density. For activity analysis, the cells were seeded in 96-well flat-bottom microtiter plates (5000 cells per well) in Dulbecco's modified Eagle's medium (Gibco) supplemented with 100 µg/ml L- Trp. Serial dilutions of both, the soluble and NP forms of rBoIFNy at quantities ranging from 6 nmol/L to 0.024 nmol/L were incubated with cells for 96 h at 37 °C. Aliquots of 160 µl of the supernatants were then mixed with 10 µl of 30 % trichloroacetic acid (T6399 Sigma-Aldrich) and incubated at 50 °C for 30 min. After a centrifugation step (10 min, 600 x *g*), aliquots of 100 µl of the supernatants were mixed with an equal volume of 4 % w/v Ehrlich´s reagent 4-(dimethylamino) benzaldehyde (156477, Sigma-Aldrich) in glacial acetic acid (Fisher Chemical A/0360/PB15). After 10 min, the absorbance at 490 nm was measured in a conventional luminometer and VICTOR3V 1420 multilabel reader (PerkinElmer).

The absorbance vs IFN-γ quantity curves were adjusted to Eq. 1. Abs*490* is the absorbance at 490 nm, which represents an indirect measurement of IFN-γ binding to the receptor, Abs*max* is the maximal binding of IFN-γ to the receptor, and K_D is the equilibrium dissociation constant. A low value of K_D indicates high IFN-γ affinity to the receptor.

$$\mathrm{Abs490} = \frac{\mathrm{Abs}max \text{ x IFN}\gamma}{\mathrm{IFN}\gamma + \mathbf{Kd}} \qquad (1)$$

2.9. Assay of protein solubilization from protein nanoparticles

The rBoIFN-γ protein NPs (rBoIFN-γ_L, rBoIFN-γ_L6K2, rBoIFN-γ_CYOB and rBoIFN-γ_HALRU) were solubilized in different volumes of PBS depending on their initial protein

295 amounts. In all cases, the concentration was adjusted to 20 μg/ml. After manual agitation,
296 every sample was incubated at 37 °C for 96 h to reproduce the conditions used during the
297 biological activity determination. The soluble and insoluble fractions were then isolated by
298 centrifugation (15 min, 15,000 x *g*). The protein amounts in the soluble fractions were
299 quantified, and the concentrations were adjusted. The biological activity of every sample
300 was determined at a single concentration (3 ng/μl) as described previously. The protein
301 released from the protein NPs was resuspended in Laemmli buffer (1x) (from Laemmli
302 buffer (4x): 1.28 g of Tris base, 8 ml of glycerol, 1.6 g of sodium dodecylsulfate (SDS), 4 ml
303 of β-mercaptoethanol and 9.6 g of urea in a final volume of 100 ml), boiled at 98 °C for
304 45 min, and loaded onto SDS–polyacrylamide gel electrophoresis (10 % acrylamide)
305 denaturing gels. Protein bands were detected by Western blot using a commercial 6xHis
306 monoclonal antibody (631212, Clontech) and a goat anti-mouse IgG (H + L)-HRP conjugate
307 (1706516, Bio-Rad) as the secondary antibody. Images of the membranes were obtained
308 using the ChemiDoc Imaging System (Bio-Rad), and bands were quantified with Image Lab
309 Software (Bio-Rad) using known concentrations of commercial rBoIFN-γ (20, 15, 10, 5, 3
310 and 1 ng; 2300-BG-025, R&D Systems).
311
312 **2.10. Interferon size determination**
313 The volume size distribution of interferon γ was determined by Dynamic Light
314 Scattering (DLS). A 60-μl aliquot (stored at -80 °C) was thawed, and the volume size
315 distribution of each protein format was immediately determined at 633 nm (Zetasizer
316 Nano ZS, Malvern Instruments Ltd.).

317

318 **2.11. Analysis of protein conformation by intrinsic tryptophan fluorescence**

319 Fluorescence spectra were recorded on a Cary Eclipse spectrofluorometer (Agilent
320 Technologies). A quartz cell with a 10-mm path length and a thermostated holder was
321 used. The excitation and emission slits were set at 5 nm. The excitation wavelength (λ_{ex})
322 was set at 295 nm. Emission spectra were acquired within a range from 310 to 550 nm.
323 The protein concentration was 0.3 mg/ml in PBS. *T*o evaluate conformational differences
324 between the proteins, we applied the CSM. CSM is the weighted average of the
325 fluorescence spectrum peak.

326 The CSM was calculated for each of the fluorescence emission spectra [58] according to
327 Eq.2, where I_i is the fluorescence intensity measured at wavelength λ_i.

328

329 $$\lambda = \frac{\sum \lambda_i . I_i}{\sum I_i} \qquad (2)$$

330

331 **2.12. Statistical analysis**

332 Prior to the use of parametric tests, normality and homogeneity of variances were
333 tested using the Shapiro-Wilk test for all quantitative data or the Levene test for raw or
334 transformed data. First, divergences between groups were tested with one-way ANOVA,
335 and pairwise comparisons were made with Student's t tests. The results were expressed
336 as the arithmetic mean for non-transformed data ± the standard error of the mean
337 ($\bar{x}$ ± SEM), except otherwise stated.

The least squares method was applied to fit functions through a regression analysis to determine the Kd values according to Eq. 1. Significance was accepted at $p < 0.05$, and Bonferroni correction was applied for sequential comparisons. All statistical analyses were performed with SPSS v. 18 for Windows.

3. Results and discussion

3.1. Production of rBoIFN-γ in *L. lactis*

The IFN-γ gene of mammalian species encodes a preproprotein of 155-166 amino acids, including a signal peptide of 22-23 amino acids and a propeptide in the last few residues, rendering a mature protein of 15.6 to 17 kDa. Heterogeneity of the C-terminus has been described, giving rise to variants of human IFN-γ ending at residues 150, 160 or 161 [59]. Human IFN-γ is usually produced in the *E. coli* expression system and is purified from IBs by using denaturing/refolding methodologies [48-50]. The same strategy has been used for mouse IFN-γ [60]. In other approaches, recombinant proteins of bovine and ovine origin are obtained from the soluble cell fraction of *E. coli* and *Corynebacterium glutamicum* [61,62]. In the present work, the mature form of bovine IFN-γ (rBoIFN-γ) protein (UniProtKB P07353, residues 24 to 166) was used as a model protein and it was produced in *L. lactis* with the aim of opening up new opportunities for novel protein production platforms. Specifically, different APPs were fused to rboIFN-γ to evaluate the ability of the peptides to increase protein aggregation and to analyze the biological activity retained in the naturally occurring protein aggregates.

359 To improve gene expression, the DNA sequence of the recombinant gene was codon
360 optimized for the *L. lactis* expression system. Three peptides, CYOB, HALRU and L6K2,
361 were selected based on their predicted aggregation propensity (Table 1 and Fig. 1a).
362 AGGRESCAN was used to identify aggregation-prone segments in proteins deposited in the
363 Disprot protein database version v6.02 [53]. CYOB was selected as the peptide displaying
364 the highest hot spot area (HSA). HALRU showed a high normalized hot spot area (NHSA)
365 and average aggregation-propensity hot spot (a^4vAHS) while maintaining a significantly
366 high HSA value relative to the other identified peptides. Finally, L6K2 was previously
367 identified as a surfactant-like peptide with the ability to enhance the aggregation
368 propensity of several proteins [55]. In the analysis, this peptide exhibited high NHSA and
369 a^4vAHS values despite having shorter sequence. A linker with a predicted random coil
370 conformation was positioned between the IFN-γ and APP as previously described [55].

371 In *L. lactis*, most of the protein was detected in the soluble cell fraction in the absence
372 of any of the APP (Fig. 1b). This observation is in agreement with previous results for the
373 expression of the natural DNA sequence of the bovine IFN-γ gene in *E. coli* in which His-
374 tagged rBoIFN-γ was purified by affinity chromatography from the soluble cell fraction
375 [62]. The presence of the APPs in the recombinant protein caused a noticeable shift of the
376 final products toward the insoluble cell fraction, as expected (Fig. 1b, bottom). The purity
377 of the protein aggregates ranged between 50-60 % in all constructs (data not shown). The
378 APP resulting in the highest aggregation tendency was the L6K2 peptide. In addition, the
379 presence of an APP tag also had a negative effect on the total recombinant protein
380 produced in the cell (Fig, 1a, top). This negative effect was maximal at 3 h, when protein

levels of 13.82 ± 2.01 μg/ml, 11.38 ± 0.36 μg/ml, and 10.36 ± 0.45 μg/ml were observed for the IFN-γ variants fused with the L6K2, HALRU and CYOB peptides, respectively, compared with 211.99 ± 51.46 μg/ml for wild type IFN-γ. Therefore, the best APP in terms of aggregation propensity and protein yield in the insoluble cell fraction, corresponded to the IFN-γ L6K2 formulation. Surprisingly, the performance of this surfactant-like peptide exceeded the predicted aggregation-prone capabilities of CYOB and HALRU peptides (Table 1).

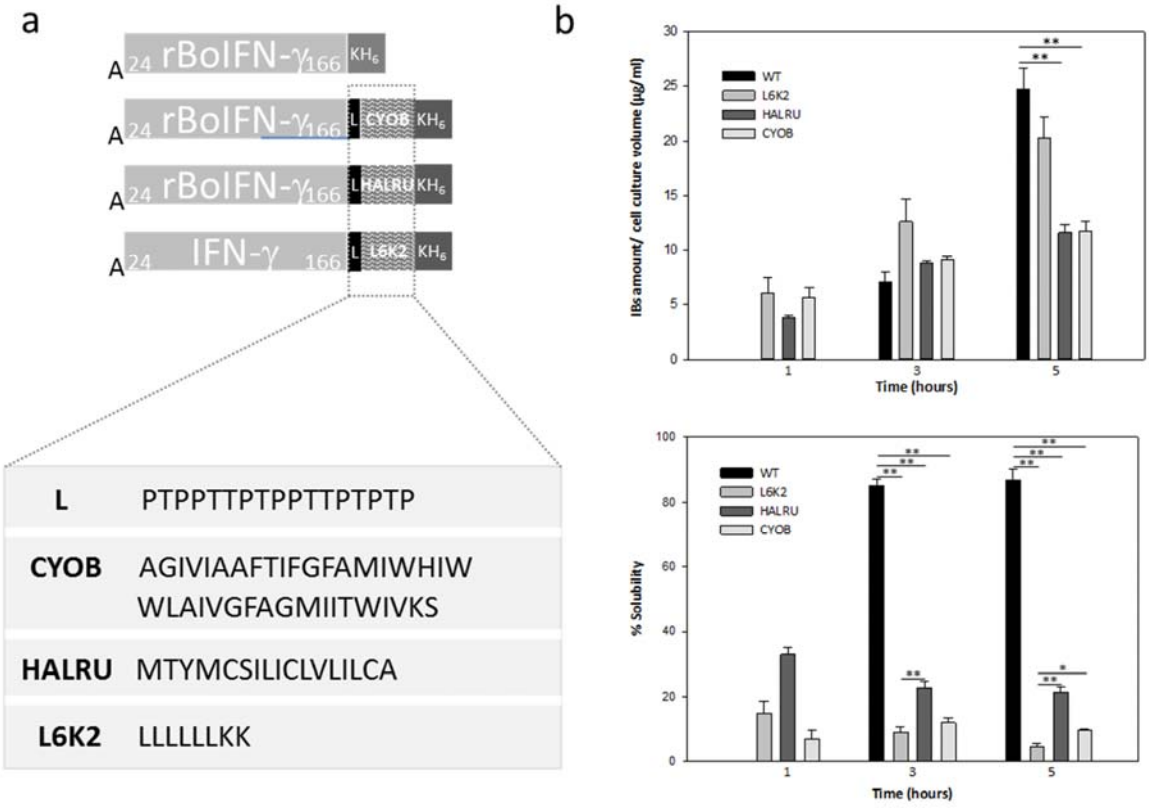

FIG 1 (a) IFN-γ constructs produced in *E. coli* and *L. lactis*. Residues of the IFN-γ protein are depicted in the corresponding light grey rectangles. APPs are indicated as wavy pattern boxes. The amino acid sequences of the APPs and the linker (black rectangles) between

bovine IFN-γ and the APPs are shown below the drawings. The H_6-tag fused to the C-terminus of all constructs is shown in dark grey. (b) Quantification of the production of IFN-γ in IB-like nanoparticles in *L. lactis* (top) and solubility (bottom) of IFN-γ in *L. lactis*. Significant results are shown as * $p \leq 0.05$ and ** $p \leq 0.005$.

3.2. Nanoarchitectonic characterization of protein nanoparticles

The morphometry of purified protein NPs of the rBoIFN-γ variants was examined by field emission scanning electron microscopy (FESEM; Fig. 2a). The images revealed the presence of multimeric complexes comprising discrete NPs in addition to isolated protein NPs (inset Fig. 2a). First, the NPs were similar to rBoIFN-γ protein NPs obtained previously in this expression system [9]. Z potential (ZP) measurements showed that all of the NPs presented negatively charged surfaces with negative values ranging from -38 to -28 mV (Fig. 2b), indicating the stability of the NP suspension. The higher values of ZP obtained for the IFN-γ variants provide information about particle stability, as NPs displaying higher ZP values (higher than +30 mV or lower than -30 mV) exhibit increased stability due to greater electrostatic repulsion between particles [63].

a

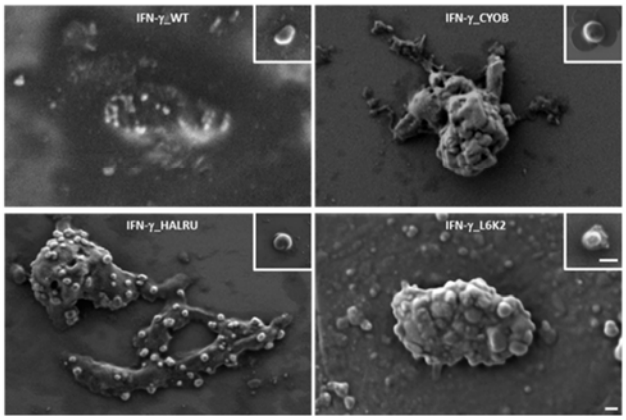

b

	Z Potential
IFN-γ	-28.46 ± 0.56 mV
IFN-γ_CYOB	-37.46 ± 0.49 mV
IFN-γ_HALRU	-37.86 ± 0.54 mV
IFN-γ_L6K2	-38.0 ± 0.65 mV

409

410 **FIG 2** (a) Ultrastructural characterization by FESEM of protein aggregates and purified
411 protein nanoparticles of rBoIFN_γ, rBoIFN- γ_CYOB, rBoIFN- γ_HARLU and rBoIFN- γ_L6K2.
412 Scale bars correspond to 200 nm. (b) Z potential of purified protein nanoparticles.

413

414 **3.3. Biological activity of soluble IFN-γ and nanoparticles of IFN-γ**

415 The activity of IFN-γ is usually determined by an antiviral assay [64]. This assay must be
416 performed in facilities with an appropriate biosafety level, and viral stocks have to be
417 maintained over time. Therefore, alternative assays have been developed to simplify the
418 procedure. One approach to evaluate IFN-γ activity mediated by IFN-γ-receptor binding is
419 the detection of kynurenine. The antiproliferative activity of IFN-γ in this assay is related to
420 the induction of the expression of the indoleamine 2,3-dioxygenase 1 (*IDO1*) gene, which
421 is the first and rate-limiting enzyme in tryptophan catabolism. IDO1 catalyzes oxidative
422 cleavage of tryptophan to N-formylkynurenine. Following a hydrolysis step, the latter is
423 transformed into kynurenine by Ehrlich's reagent, giving a yellow-colored compound

absorbing at 490 nm [65]. The activity of IFN-γ is highly species-specific and the detection of tryptophan hydrolysis by IDO1 has been then stablished for different cell lines, including bovine cells [57]. Thus, a specific assay for the bovine IFN-γ was developed and validated in this study. For the validation process of the developed procedure, the activity of three soluble rBoIFN-γ proteins was tested (Fig. 3a). rBoIFN-γ_Std exhibited the lowest dissociation constant (K_D) among the proteins purified from the soluble cell fraction (Fig. 3a). The difference in this parameter with in-house IFN-γ produced in *Clearcoli* (rBoIFN-γ_*E. coli*) may be related to the absence of C-terminal variants in this sample or the effect of the fused His-tag to the C-term although may also be attributable to other variables [66]. The protein obtained from the *L. lactis* expression system displayed less activity, which may be to differences in the production process among prokaryotic expression systems [67,68]. Once the activity assay was validated, the biological activity contained in the IFN-γ protein NPs produced in *L. lactis* was determined. For that, bovine cells were incubated with increasing amounts of rBoIFN-γ NPs, that is, protein NPs purified from the insoluble cell fraction (Fig. 3b). The results showed that all cells were able to elicit responses to the presence of the protein NPs, and the IFN-γ_L6K2 formulation displayed the highest initial rate and kynurenine production. The addition of HALRU and CYOB APP to IFN-γ had a moderate effect on the cell response. As shown in Fig. 3a and Fig. 3b, the experiments were performed at the same time with the same stock of cells and conditions. We wondered why the sample corresponding to protein NPs of IFN-γ_L6K2 had the highest activity and initial rate, even compared with commercial IFN-γ. Consistent with this observation, a previous analysis of the activity of recombinant β-galactosidase

446 produced in *E. coli* in the form of protein NPs revealed higher specific activity than the
447 corresponding soluble version of the protein [21]. However, these protein NPs obtained
448 from *E. coli* have not been characterized in detail. The activity displayed by IBs produced in
449 *E. coli* has been attributed to the release of a spectrum of conformers of the recombinant
450 protein, which leaves a scaffold that is resistant to proteolysis and has an extensive cross-
451 beta-pleated sheet conformation [69,70]. In fact, in the case of protein NPs of rBoIFN-γ
452 produced in *L. lactis*, 30-40 % of the material is resistant to proteolysis, indicating that the
453 protein NPs obtained in this expression system follow the same principles as the *E. coli*
454 system [9]. Therefore, the activities displayed by the protein NPs are probably due to the
455 partial release of the IFN-γ that forms part of the macromolecular complex [27]. To better
456 evaluate the ability of the protein NPs to release protein, they were incubated in PBS for
457 96 h to emulate the protein release conditions established during the biological activity
458 assay of the protein NPs (see the experimental design used to obtain the different protein
459 samples in Fig. 3c). Release of 52.67 %, 5.30 %, 0.42 % and 0.46 % was observed for IFN-γ,
460 IFN-γ_L6K2, IFN-γ_HALRU and IFN-γ_CYOB NPs, respectively. Aiming to analyze the specific
461 activity of the proteins released from the protein NPs, an activity assay was performed
462 and the results were compared with soluble proteins obtained directly from the soluble
463 cell fraction (Fig. 3d). The results showed that the maximal specific activity corresponded
464 to the IFN-γ_L6K2 protein released from NPs. In addition, the comparison of the specific
465 activity of the rBoIFN-γ protein produced in *L. lactis* and purified from the soluble cell
466 fraction with that of the corresponding protein released from NPs showed that the

released protein elicited better conformational performance (compare the second and last bars in Fig. 3d).

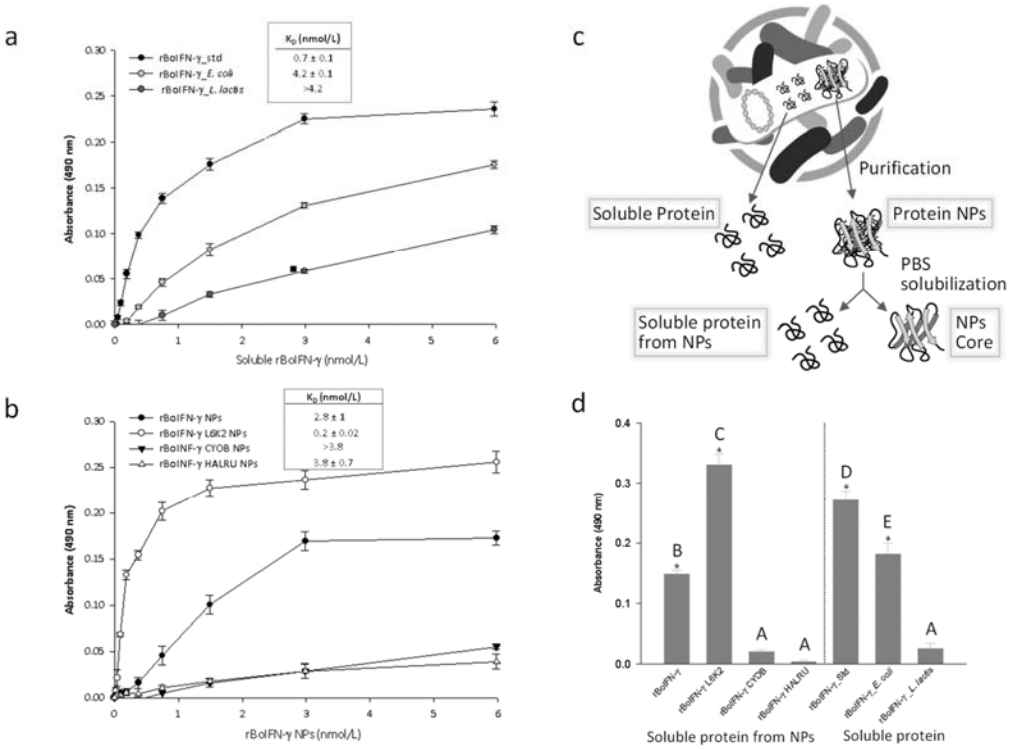

FIG 3 Kynurenine levels measured by absorbance at 490 nm after treatment of EBTr cells for 96 h with increasing amounts of rBoIFN-γ from different origins. (a) Soluble rBoIFN-γ produced in the indicated expression system. (b) Protein nanoparticles of rBoIFN-γ produced in *L. lactis*. The Kd values are indicated in the plot. (c) Schematic representation of the protein samples used in the activity assays: soluble protein obtained from the soluble cell fraction, protein NPs purified from the insoluble cell fraction, soluble protein obtained from the protein NPs, and the NP core after a resolubilization procedure. (d) Comparison of the activity between rBoIFN-γ protein obtained from solubilization of protein NPs and purified rBoIFN-γ from the soluble cell fraction as indicated at 0.72

479 nmol/L. Different letters depict differences between proteins ($p < 0.001$) except rBoIFN-γ
480 from protein NPs and rBoIFN-γ_E ($p = 0.024$).

481 In this context, the addition of APPs to the rBoIFN-γ protein improved the aggregation
482 profile of the produced protein (Fig. 1b). However, the presence of this type of peptides
483 had a negative effect on the overall production of the protein and, in the case of HALRU
484 and CYOB, a huge impact on biological activity (Fig. 3). Therefore, AGGRESCAN software is
485 able to predict the propensity to aggregate of the resulting APP-containing recombinant
486 IFN-γ and is a reliable tool for analyzing solubility performance in the design of
487 recombinant genes [54].

488

489 **3.4. Physico-chemical characterization of soluble IFN-γ and nanoparticles of IFN-γ**

490 The precise physico-chemical analysis of recombinant proteins is important due to
491 safety concerns, and specific regulatory guidelines were redesigned for protein-based
492 pharmaceuticals after the TGN1412 clinical trial [71,72]. Therefore, the physico-chemical
493 characterization of recombinant proteins needs to be further developed, and technical
494 approaches to obtain reliable data on the quality of the final product are needed.

495 To further analyze the protein in different formats, DLS measurements were performed
496 (Fig. 4a-4d). The commercial bovine IFN-γ exhibited a peak with a maximum at 7.6 nm,
497 was quite similar to the peak at 6.13 nm for the in-house version of IFN-γ produced in *L.*
498 *lactis*. This configuration might correspond to the dimeric form of the cytokine. However,

499 the IFN-γ obtained in-house in *E. coli* showed a tendency towards a larger size. Therefore,
500 the specific activity of the different rBoIFN-γ formats is not directly linked to the dimeric
501 configuration, which is the functional conformation when binding to the cell receptor, and
502 some other variables might be involved. When analyzing the size of the purified NPs, a
503 peak above 1,000 nm was detected, which is above the upper sensitivity limit of the
504 equipment (Fig. 4b). The NPs were clustered in higher-order complexes from monomeric
505 versions of 200 nm (Fig. 2a). All samples exhibited the same profile. After solubilization of
506 the protein embedded in the NPs, the size of the remaining material remained above
507 1,000 nm since the scaffold of the NPs retained the overall structure after the protein was
508 released (Fig. 4d). The released protein showed a narrow dispersion ranging from the
509 dimeric size of the protein identified in the samples obtained from the commercial IFN-γ
510 or the soluble version purified from *L. lactis* detected in the upper panel of Fig. 4a (Fig. 4c).
511 In addition, the polydispersity index (PI) of these samples was higher than that of the
512 soluble IFN-γ versions. The PI corresponds to an estimate of the width of the distribution,
513 and the higher values of PI are in accordance with the data showing the presence of a pool
514 of conformers in the folding of recombinant proteins when the proteins are produced in
515 the cell. By contrast, in the protein versions purified from the soluble cell fraction, the
516 downstream process selects only a narrow collection of conformers, indicating that the
517 protein obtained during solubilization assays from protein NPs is more representative of
518 the diversity in conformations of a single protein that are produced in the expression
519 system.

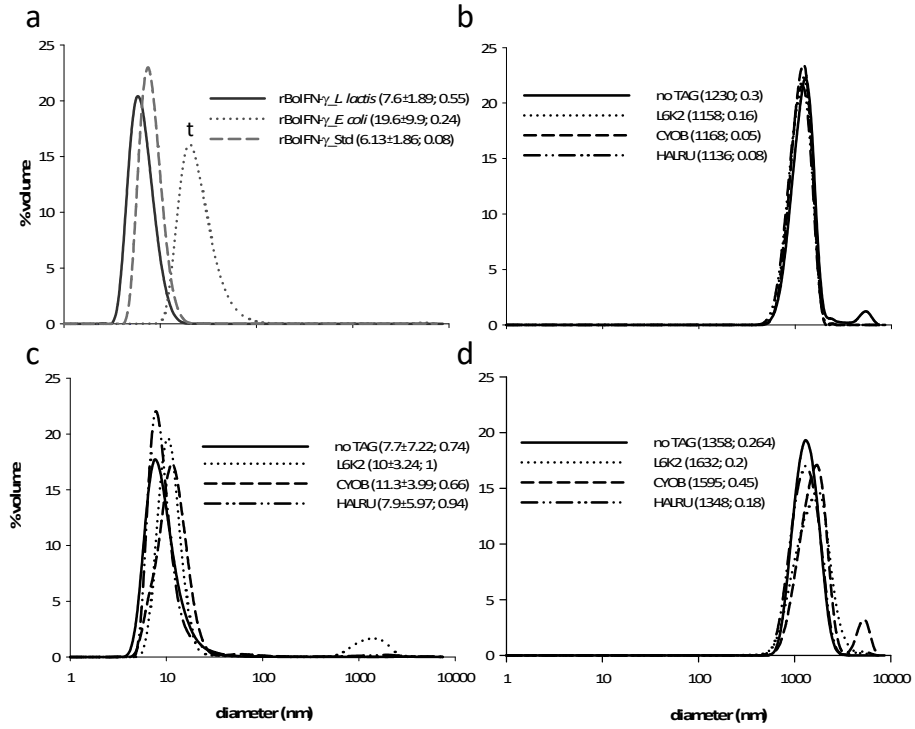

520

521 **FIG 4** Recombinant IFN-γ sizes in different supramolecular arrangements (purified soluble
522 IFN-γ and INF-γ IBs). (a) Soluble rBoIFN-γ from different origins: commercial rBoIFN-γ_Std,
523 in-house rBoIFN-γ from *E. coli* and *L. lactis*. (b) rBoIFN-γ IBs produced in *L. lactis*. (c) PBS
524 solubilized rBoIFN-γ from IBs after interferon release. (d) Scaffold of rBoIFN-γ IBs
525 incubated for 96 hours at 37 °C. The mean size and polydispersity index are indicated in
526 brackets. The average size data of the soluble proteins were analyzed by one-way ANOVA
527 (^{t} corresponds to $P < 0.07$).

528 To further analyze the link between the physico-chemical properties and the specific
529 activity of the proteins, the fluorescence emission of Trp was recorded. Each fluorescence
530 emission spectrum was transformed into a center of spectral mass (CSM) value. This
531 parameter is related to the relative exposure of the Trp to the protein environment. The

maximum red-shift in the CSM of the Trp spectrum is compatible with large solvent accessibility [73-75]. By contrast, the blue shift in the CSM corresponds to a Trp hidden in a more hydrophobic milieu [76]. The mature form of BoIFN-γ has a unique Trp. This Trp residue is partially buried in the 3D structure of the protein (PDB 1D9C) [77] and is not involved in either monomer or in cytokine-receptor interactions, as shown in the 3D structure of the human tetrameric complex of the cytokine dimer with the receptor (PDB 1FG9) [78]. A remarkable aspect of the intrinsic fluorescence analysis is that all of the rBoIFN-γ variants within the NPs or after solubilization from the protein NPs exhibited lower CSM values than the samples obtained from the soluble fraction (Table 2). These results suggest that the protein forming part of the NPs and the protein solubilized from the aggregates have a more compact conformation than the soluble version. The differences between the soluble IFN-γ versions are due to differences in protein origin, sequence and size. The most efficient IFN-γ soluble version corresponded to the commercial IFN-γ, which had the lowest CMS due to its highly compacted structure. The proteins obtained from the soluble fraction of *E. coli* and *L. lactis* exhibited higher CMS values than the commercial protein. These differences might be related to the distinct sizes detected (Fig. 4a). The in-house rBoIFN-γ_*E. coli* was approximately three times larger than the same NPs produced in *L lactis*, indicating that the Trp residue sensed a more polar environment compared with the *L lactis* form (Table 2). Interestingly, for the protein originating from the particulate form, a blue shift was observed compared with the soluble versions, and the CSM increased as it was resolubilized (lines 2 and 4 of Table 2), at least in versions with a percentage of release above 5 %. Interestingly, the CSM

554 value of the PBS solubilized rBoIFN-γ_*L. lactis* protein sample did not reach that of the
555 soluble counterpart (lines 3 and 4 of Table 2). When the APPs were incorporated in the
556 engineered protein constructs, the solubilized proteins showed a decrease in the CSM
557 values compared with the protein NPs samples (lines 5 and 7). This behavior suggests a
558 possible self-arrangement of the tag within the protein that could replace water molecules
559 and increase the hydrophobicity of the Trp environment. The CYOB construct (line 6 of
560 Table 2) required a specific analysis as this tag contributes five additional Trp residues to
561 the whole protein structure. In this case, the solubilized protein spectrum exhibited a
562 modest red shift (higher CMS value) compared with the particulate form, indicating that
563 the solubilization process exposed some of the Trp residues to a hydrophilic environment.
564 The CSM values of the CYOB and HALRU protein NPs remained unaltered after
565 solubilization (Table 2, lines 6 and 7). These data are in accordance with the higher
566 stability of the particulate forms, which exhibited low levels of protein release.

567 The NP form of IFN-γ also favored the specific activity (insets, Fig. 3, *L. lactis* and non-
568 tagged rBoIFN). This phenomenon is not only due to more active conformation of the
569 protein (Fig. 4 and Table 2, line 3 vs line 4) [79] but also to the heterogeneous distribution
570 of the protein and the ability of the protein NPs to increase the effective concentration of
571 protein in the proximity of the receptor. Moreover, the formulation containing L6K2 was
572 the most efficient, even compared with the commercial protein. Solubilization clearly
573 conferred the most active and altered conformation of the protein without the tag.
574 Although a low percentage of protein was released from the NPs containing L6K2, at least

575 in the physiological buffer PBS, this released protein seems to be sufficient to surpass the
576 activity of the released protein without a tag (Fig.3).

577 Another interesting aspect is the effect of the size of the tag on the structure-function
578 of the protein. The incorporation of a tag larger than 17 aa beyond the linker (Fig. 1a)
579 could generate steric problems preventing the interaction of tagged IFN-γ with the
580 receptor. The larger the tag, the more negative the effect on the activity is detected. As
581 shown in Fig. 1, L6K2 is only 8 aa, compared with 17 aa for HALRU and 38 aa for CYOB. The
582 short size of the L6K2 tag might reduce the difficulty of the interaction between L6K2-IFN-
583 γ and the receptor compared with the longer IFN-γ tags.

584 The size of the APP is an important parameter, and as a general rule, the longer the
585 aggregation peptide, the higher the HSA. However, small peptides with a discrete HSA but
586 high normalized and average HSA have also been reported to enhance the aggregation of
587 the accompanying proteins, as in the case of L6K2 [55]. Surprisingly, the L6K2 peptide also
588 leads to the production of highly active protein in the protein NPs. The detailed physico-
589 chemical characterization of the protein samples revealed higher compactability of the
590 protein conformations in the protein samples with the highest biological activity. The
591 protein peaks of the soluble protein samples indicated that the purification strategy of a
592 protein selects for a narrower distribution of protein conformations compared with
593 protein samples recovered from naturally occurring protein NPs (compare the PDI of the
594 samples obtained from the soluble cell fraction with the protein samples obtained after
595 solubilization of protein NPs in Fig. 4).

In the recombinant protein production platform, the general consensus for improving protein yield is to improve the solubility of the protein. Consequently, the major established strategies for producing recombinant protein involve improving solubility by including folding modulators or reducing the growth rate. However, solubility and conformational quality are not necessarily coincident parameters [80]. The functionalities of the protein obtained from the soluble cell fraction or the protein NPs of rBoIFN-γ_*L. lactis* in the present work were in accordance with these previous findings, as the protein obtained from the soluble cell fraction was less active than that recovered from the protein NPs. The compactabilities of the conformations of these proteins were in agreement with their dissimilar biological activity. The results obtained in this study are in accordance with previous analyses indicating that the compactability of protein conformations is a key parameter related to stability and function [81,82].

Consistent with these observations, the addition of the L6K2 APP to rBoIFN-γ_*L. lactis* improved the biological performance of the resulting conformational species retained in the corresponding protein NPs. Interestingly, this APP showed higher capability as a compactability factor compared with the other APPs tested with IFN-γ. In fact, the addition of the other two APPs to rBoIFN-γ (HALRU and CYOB) surprisingly had negative effects on the functionality of the resulting proteins, despite levels of compactability similar to that of the protein sample lacking the APPs. These sequences might have negative effects by preventing correct binding of the dimer to the cell receptor. In conclusion, the detailed physico-chemical characterization of the purified recombinant

617 proteins needs to be further developed to select a more appropriate product to optimize
618 the quality of the recombinant product.

619

620 **4. Conclusions**

621 The demand for recombinant proteins in the pharmaceutical industry is steadily
622 increasing. Emerging novel protein formulations, including naturally occurring protein NPs,
623 might be an alternative to soluble variants for fine analysis at the biophysical level. Such
624 analyses are important to address safety about biological molecules.

625 This study analyzes the effect of aggregation-prone peptides (APPs) on the improvement
626 of the production of naturally occurring protein nanoparticles (NPs) of interferon gamma
627 (IFN-γ) in the generally recognized as safe (GRAS) *Lactococcus lactis* expression system. In
628 addition, the fine physico-chemical characterization of the resulting proteins, either
629 obtained from the soluble or insoluble cell fractions, indicates that the selected
630 engineered proteins embedded in the protein NPs show higher compactability than their
631 soluble protein counterparts. Conformational compactability is directly related to the
632 biological performance of the recombinant IFN-γ. This data prompt us to further explore
633 the relationship between compactability of protein conformations and protein quality in
634 naturally occurring protein NPs, envisioned as protein depots for the controlled release of
635 therapeutic proteins for biomedical applications.

636

Acknowledgments

This work was supported by grants from INIA, MINECO, Spain to N.F.M. and E.G.F. (RTA2015-00064-C02-01 and RTA2015-00064-C02-02). The authors acknowledge financial support granted to A.V. from AGAUR (2017 SGR-229) and from the Centro de Investigación Biomédica en Red (CIBER) de Bioingeniería, Biomateriales y Nanomedicina financed by the Instituto de Salud Carlos III with assistance from the European Regional Development. We are also indebted to the CERCA Programme (Generalitat de Catalunya) and European Social Fund for supporting our research. J.V.C. received a pre-doctoral fellowship from UAB, O.C.G. received a PhD fellowship from MECD (FPU), and E.G.F. received a post-doctoral fellowship from INIA (DOC-INIA). AV has been distinguished with an ICREA ACADEMIA Award. The authors also acknowledge ICTS ‘‘NANBIOSIS”, more specifically the Protein Production Platform of CIBER in Bioengineering, Biomaterials & Nanomedicine (CIBER- BBN)/IBB, at the UAB sePBioEs scientific-technical service (http://www.nanbiosis.es/unit/u1-protein-production-platform-ppp/) and the UAB scientific-technical services LLEB, SM and SCAC (https://www.uab.cat/web/research/scientific-technical-services/all-scientific-technical-services--1345667278676.html). The authors would like to thank Milena Tileva for her helpful advice on technical issues related to the experimental adjustment of the IFN-γ activity bioassay. Special thanks to Sandra Párraga-Ferrer for the design of Fig. 3c. E. Garcia-Fruitós and N. Ferrer-Miralles designed and supervised the experiments. J.V. Carratalà, O. Cano-Garrido, J. Sánchez, C. Membrado, E. Pérez, O. Conchillo-Solé and A. Sánchez-Chardi performed the experiments. J. V. Carratalà, O. Cano-Garrido, J. Sánchez

and N. Ferrer-Miralles analyzed the data. All authors edited the manuscript. N. Ferrer-Miralles wrote the paper.

References

[1] M.N. Baeshen, A.M. Al-Hejin, R.S. Bora, M.M. Ahmed, H.A. Ramadan, K.S. Saini, N.A. Baeshen, E.M. Redwan, Production of Biopharmaceuticals in E. coli: Current Scenario and Future Perspectives, J Microbiol Biotechnol 25 (2015) pp. 953-962. https://doi.org/10.4014/jmb.1412.12079.

[2] L. Sanchez-Garcia, L. Martin, R. Mangues, N. Ferrer-Miralles, E. Vazquez, A. Villaverde, Recombinant pharmaceuticals from microbial cells: a 2015 update, Microb Cell Fact 15 (2016) p.33. https://doi.org/10.1186/s12934-016-0437-3.

[3] P.O. Magalhaes, A.M. Lopes, P.G. Mazzola, C. Rangel-Yagui, T.C. Penna, A. Pessoa, Jr., Methods of endotoxin removal from biological preparations: a review, J Pharm. Pharm. Sci 10 (2007) pp. 388-404.

[4] D. Petsch and F.B. Anspach, Endotoxin removal from protein solutions, J Biotechnol 76 (2000) pp. 97-119.

[5] F. Rueda, M.V. Cespedes, A. Sanchez-Chardi, J. Seras-Franzoso, M. Pesarrodona, N. Ferrer-Miralles, E. Vazquez, U. Rinas, U. Unzueta, U. Mamat, R. Mangues, E. Garcia-Fruitos, A. Villaverde, Structural and functional features of self-assembling protein nanoparticles produced in endotoxin-free Escherichia coli, Microb Cell Fact 15 (2016) p.59. 10.1186/s12934-016-0457-z [doi];10.1186/s12934-016-0457-z [pii].

[6] U. Mamat, K. Wilke, D. Bramhill, A.B. Schromm, B. Lindner, T.A. Kohl, J.L. Corchero, A. Villaverde, L. Schaffer, S.R. Head, C. Souvignier, T.C. Meredith, R.W. Woodard, Detoxifying Escherichia coli for endotoxin-free production of recombinant proteins, Microb Cell Fact 14 (2015) p.57. 10.1186/s12934-015-0241-5 [doi];10.1186/s12934-015-0241-5 [pii].

[7] A.A. Song, L.L.A. In, S.H.E. Lim, R.A. Rahim, A review on Lactococcus lactis: from food to factory, Microb Cell Fact 16 (2017) p.55. 10.1186/s12934-017-0669-x [doi];10.1186/s12934-017-0669-x [pii].

689 [8] E. Garcia-Fruitos, Lactic Acid Bacteria: a promising alternative for recombinant
690 protein production, Microb Cell Fact 11 (2012) p.157. 1475-2859-11-157
691 [pii];10.1186/1475-2859-11-157 [doi].

692 [9] O. Cano-Garrido, A. Sanchez-Chardi, S. Pares, I. Giro, W.I. Tatkiewicz, N. Ferrer-
693 Miralles, I. Ratera, A. Natalello, R. Cubarsi, J. Veciana, A. Bach, A. Villaverde, A. Aris,
694 E. Garcia-Fruitos, Functional protein-based nanomaterial produced in
695 microorganisms recognized as safe: A new platform for biotechnology, Acta
696 Biomater. 43 (2016) pp. 230-239. https://doi.org/10.1016/j.actbio.2016.07.038.

697 [10] N. Ferrer-Miralles and A. Villaverde, Bacterial cell factories for recombinant
698 protein production; expanding the catalogue, Microb Cell Fact 12 (2013) p.113.
699 https://doi.org/10.1186/1475-2859-12-113.

700 [11] R.R. Kopito, Aggresomes, inclusion bodies and protein aggregation, Trends Cell
701 Biol 10 (2000) pp. 524-530.

702 [12] U. Rinas, E. Garcia-Fruitos, J.L. Corchero, E. Vazquez, J. Seras-Franzoso, A.
703 Villaverde, Bacterial Inclusion Bodies: Discovering Their Better Half, Trends
704 Biochem Sci 42 (2017) pp. 726-737. https://doi.org/10.1016/j.tibs.2017.01.005.

705 [13] E. Rodriguez-Carmona, R. Mendoza, E. Ruiz-Canovas, N. Ferrer-Miralles, I. Abasolo,
706 Schwartz S Jr, A. Villaverde, J.L. Corchero, A novel bio-functional material based on
707 mammalian cell aggresomes, Appl. Microbiol Biotechnol 99 (2015) pp. 7079-7088.
708 https://doi.org/10.1007/s00253-015-6684-0.

709 [14] G.L. Rosano and E.A. Ceccarelli, Recombinant protein expression in Escherichia
710 coli: advances and challenges, Front Microbiol 5 (2014) p.172.
711 https://doi.org/10.3389/fmicb.2014.00172.

712 [15] H.P. Sorensen and K.K. Mortensen, Soluble expression of recombinant proteins in
713 the cytoplasm of Escherichia coli, Microb Cell Fact 4 (2005) p.1.
714 https://doi.org/10.1186/1475-2859-4-1.

715 [16] S. Peternel and R. Komel, Active protein aggregates produced in Escherichia coli,
716 Int J Mol Sci 12 (2011) pp. 8275-8287. https://doi.org/10.3390/ijms12118275.

717 [17] E. Garcia-Fruitos, Inclusion bodies: a new concept, Microb Cell Fact 9 (2010) p.80.
718 https://doi.org/10.1186/1475-2859-9-80.

719 [18] B. Jurgen, A. Breitenstein, V. Urlacher, K. Buttner, H. Lin, M. Hecker, T. Schweder,
720 P. Neubauer, Quality control of inclusion bodies in Escherichia coli, Microb Cell
721 Fact 9 (2010) p.41. https://doi.org/10.1186/1475-2859-9-41.

[19] A. Singh, V. Upadhyay, A.K. Upadhyay, S.M. Singh, A.K. Panda, Protein recovery from inclusion bodies of Escherichia coli using mild solubilization process, Microb Cell Fact 14 (2015) p.41. https://doi.org/10.1186/s12934-015-0222-8.

[20] H. Yamaguchi and M. Miyazaki, Refolding techniques for recovering biologically active recombinant proteins from inclusion bodies, Biomolecules. 4 (2014) pp. 235-251. https://doi.org/10.3390/biom4010235.

[21] E. Garcia-Fruitos, N. Gonzalez-Montalban, M. Morell, A. Vera, R.M. Ferraz, A. Aris, S. Ventura, A. Villaverde, Aggregation as bacterial inclusion bodies does not imply inactivation of enzymes and fluorescent proteins, Microb Cell Fact 4 (2005) p.27. https://doi.org/10.1186/1475-2859-4-27.

[22] S. Jevsevar, V. Gaberc-Porekar, I. Fonda, B. Podobnik, J. Grdadolnik, V. Menart, Production of nonclassical inclusion bodies from which correctly folded protein can be extracted, Biotechnol Prog. 21 (2005) pp. 632-639. https://doi.org/10.1021/bp0497839.

[23] J. Nahalka and B. Nidetzky, Fusion to a pull-down domain: a novel approach of producing Trigonopsis variabilisD-amino acid oxidase as insoluble enzyme aggregates, Biotechnol Bioeng. 97 (2007) pp. 454-461. https://doi.org/10.1002/bit.21244.

[24] L. Gifre-Renom, O. Cano-Garrido, F. Fabregas, R. Roca-Pinilla, J. Seras-Franzoso, N. Ferrer-Miralles, A. Villaverde, A. Bach, M. Devant, A. Aris, E. Garcia-Fruitos, A new approach to obtain pure and active proteins from Lactococcus lactis protein aggregates, Sci Rep. 8 (2018) p.13917. 10.1038/s41598-018-32213-8 [doi];10.1038/s41598-018-32213-8 [pii].

[25] E. Vazquez, J.L. Corchero, J.F. Burgueno, J. Seras-Franzoso, A. Kosoy, R. Bosser, R. Mendoza, J.M. Martinez-Lainez, U. Rinas, E. Fernandez, L. Ruiz-Avila, E. Garcia-Fruitos, A. Villaverde, Functional inclusion bodies produced in bacteria as naturally occurring nanopills for advanced cell therapies, Adv Mater. 24 (2012) pp. 1742-1747. 10.1002/adma.201104330 [doi].

[26] M.V. Cespedes, Y. Fernandez, U. Unzueta, R. Mendoza, J. Seras-Franzoso, A. Sanchez-Chardi, P. Alamo, V. Toledo-Rubio, N. Ferrer-Miralles, E. Vazquez, S. Schwartz, I. Abasolo, J.L. Corchero, R. Mangues, A. Villaverde, Bacterial mimetics of endocrine secretory granules as immobilized in vivo depots for functional protein drugs, Sci Rep. 6 (2016) p.35765. https://doi.org/10.1038/srep35765.

[27] U. Unzueta, M.V. Cespedes, R. Sala, P. Alamo, A. Sanchez-Chardi, M. Pesarrodona, L. Sanchez-Garcia, O. Cano-Garrido, A. Villaverde, E. Vazquez, R. Mangues, J. Seras-Franzoso, Release of targeted protein nanoparticles from functional bacterial

758 amyloids: A death star-like approach, J Control Release 279 (2018) pp. 29-39.
759 https://doi.org/10.1016/j.jconrel.2018.04.004.

760 [28] J. Seras-Franzoso, C. Steurer, M. Roldan, M. Vendrell, C. Vidaurre-Agut, A.
761 Tarruella, L. Saldana, N. Vilaboa, M. Parera, E. Elizondo, I. Ratera, N. Ventosa, J.
762 Veciana, A.J. Campillo-Fernandez, E. Garcia-Fruitos, E. Vazquez, A. Villaverde,
763 Functionalization of 3D scaffolds with protein-releasing biomaterials for
764 intracellular delivery, J Control Release 171 (2013) pp. 63-72.
765 https://doi.org/10.1016/j.jconrel.2013.06.034.

766 [29] J. Seras-Franzoso, K. Peebo, E. Garcia-Fruitos, E. Vazquez, U. Rinas, A. Villaverde,
767 Improving protein delivery of fibroblast growth factor-2 from bacterial inclusion
768 bodies used as cell culture substrates, Acta Biomater. 10 (2014) pp. 1354-1359.
769 https://doi.org/10.1016/j.actbio.2013.12.021.

770 [30] U. Krauss, V.D. Jager, M. Diener, M. Pohl, K.E. Jaeger, Catalytically-active inclusion
771 bodies-Carrier-free protein immobilizates for application in biotechnology and
772 biomedicine, J Biotechnol 258 (2017) pp. 136-147.
773 https://doi.org/10.1016/j.jbiotec.2017.04.033.

774 [31] K. Schroder, P.J. Hertzog, T. Ravasi, D.A. Hume, Interferon-gamma: an overview of
775 signals, mechanisms and functions, J Leukoc. Biol 75 (2004) pp. 163-189.
776 https://doi.org/10.1189/jlb.0603252.

777 [32] P.C. Le, P. Genin, M.G. Baines, J. Hiscott, Interferon activation and innate
778 immunity, Rev. Immunogenet. 2 (2000) pp. 374-386.

779 [33] J.R. Schoenborn and C.B. Wilson, Regulation of interferon-gamma during innate
780 and adaptive immune responses, Adv Immunol. 96 (2007) pp. 41-101.
781 https://doi.org/10.1016/S0065-2776(07)96002-2.

782 [34] A. Razaghi, L. Owens, K. Heimann, Review of the recombinant human interferon
783 gamma as an immunotherapeutic: Impacts of production platforms and
784 glycosylation, J Biotechnol 240 (2016) pp. 48-60.
785 https://doi.org/10.1016/j.jbiotec.2016.10.022.

786 [35] K. Jiang, S. Cao, J.Z. Cui, J.A. Matsubara, Immuno-modulatory Effect of IFN-gamma
787 in AMD and its Role as a Possible Target for Therapy, J Clin Exp. Ophthalmol. Suppl
788 2 (2013) pp. 0071-0076. https://doi.org/10.4172/2155-9570-S2-007.

789 [36] C. Kosmidis, K. Sapalidis, T. Koletsa, M. Kosmidou, C. Efthimiadis, G. Anthimidis, N.
790 Varsamis, N. Michalopoulos, C. Koulouris, S. Atmatzidis, L. Liavas, T.M. Strati, G.
791 Koimtzis, A. Tsakalidis, S. Mantalovas, K. Zarampouka, M. Florou, D.E. Giannakidis,
792 E. Georgakoudi, S. Baka, P. Zarogoulidis, Y.G. Man, I. Kesisoglou, Interferon-
793 gamma and Colorectal Cancer: an up-to date, J Cancer 9 (2018) pp. 232-238.
794 https://doi.org/10.7150/jca.22962.

795 [37] B.E. Marciano, R. Wesley, E.S. De Carlo, V.L. Anderson, L.A. Barnhart, D. Darnell,
796 H.L. Malech, J.I. Gallin, S.M. Holland, Long-term interferon-gamma therapy for
797 patients with chronic granulomatous disease, Clin Infect. Dis. 39 (2004) pp. 692-
798 699. https://doi.org/10.1086/422993.

799 [38] S.M. Rowe, D.S. Borowitz, J.L. Burns, J.P. Clancy, S.H. Donaldson, G. Retsch-Bogart,
800 S.D. Sagel, B.W. Ramsey, Progress in cystic fibrosis and the CF Therapeutics
801 Development Network, Thorax 67 (2012) pp. 882-890.
802 https://doi.org/10.1136/thoraxjnl-2012-202550.

803 [39] L. Seyer, N. Greeley, D. Foerster, C. Strawser, S. Gelbard, Y. Dong, K. Schadt, M.G.
804 Cotticelli, A. Brocht, J. Farmer, R.B. Wilson, D.R. Lynch, Open-label pilot study of
805 interferon gamma-1b in Friedreich ataxia, Acta Neurol. Scand. 132 (2015) pp. 7-15.
806 https://doi.org/10.1111/ane.12337.

807 [40] G.C. Smaldone, Repurposing of gamma interferon via inhalation delivery, Adv Drug
808 Deliv. Rev. (2018). https://doi.org/10.1016/j.addr.2018.06.004.

809 [41] C.C. Wu, M.J. Econs, L.A. DiMeglio, K.L. Insogna, M.A. Levine, P.J. Orchard, W.P.
810 Miller, A. Petryk, E.T. Rush, D.M. Shoback, L.M. Ward, L.E. Polgreen, Diagnosis and
811 Management of Osteopetrosis: Consensus Guidelines From the Osteopetrosis
812 Working Group, J Clin Endocrinol. Metab 102 (2017) pp. 3111-3123.
813 https://doi.org/10.1210/jc.2017-01127.

814 [42] D.S. Green, A.T. Nunes, V. David-Ocampo, I.B. Ekwede, N.D. Houston, S.L. Highfill,
815 H. Khuu, D.F. Stroncek, S.M. Steinberg, K.C. Zoon, C.M. Annunziata, A Phase 1 trial
816 of autologous monocytes stimulated ex vivo with Sylatron((R)) (Peginterferon alfa-
817 2b) and Actimmune((R)) (Interferon gamma-1b) for intra-peritoneal administration
818 in recurrent ovarian cancer, J Transl. Med 16 (2018) p.196.
819 https://doi.org/10.1186/s12967-018-1569-5.

820 [43] D. Grimaldi, O. Pradier, R.S. Hotchkiss, J.L. Vincent, Nivolumab plus interferon-
821 gamma in the treatment of intractable mucormycosis, Lancet Infect. Dis. 17 (2017)
822 p.18. https://doi.org/10.1016/S1473-3099(16)30541-2.

823 [44] S.J. Harris, J. Brown, J. Lopez, T.A. Yap, Immuno-oncology combinations: raising
824 the tail of the survival curve, Cancer Biol Med 13 (2016) pp. 171-193.
825 https://doi.org/10.20892/j.issn.2095-3941.2016.0015.

826 [45] V. Janardhana, M.E. Ford, M.P. Bruce, M.M. Broadway, T.E. O'Neil, A.J. Karpala, M.
827 Asif, G.F. Browning, K.A. Tivendale, A.H. Noormohammadi, J.W. Lowenthal, A.G.
828 Bean, IFN-gamma enhances immune responses to E. coli infection in the chicken, J
829 Interferon Cytokine Res 27 (2007) pp. 937-946.
830 https://doi.org/10.1089/jir.2007.0020.

[46] L.K. Fox, H.D. Liggit, T. Yilma, L.B. Corbeil, The effect of interferon-gamma intramammary administration on mammary phagocyte function, Zentralbl. Veterinarmed. B 37 (1990) pp. 28-30.

[47] L. Gifre, A. Aris, A. Bach, E. Garcia-Fruitos, Trends in recombinant protein use in animal production, Microb Cell Fact 16 (2017) p.40. 10.1186/s12934-017-0654-4 [doi];10.1186/s12934-017-0654-4 [pii].

[48] R. Khalilzadeh, S.A. Shojaosadati, N. Maghsoudi, J. Mohammadian-Mosaabadi, M.R. Mohammadi, A. Bahrami, N. Maleksabet, M.A. Nassiri-Khalilli, M. Ebrahimi, H. Naderimanesh, Process development for production of recombinant human interferon-gamma expressed in Escherichia coli, J Ind Microbiol Biotechnol 31 (2004) pp. 63-69. https://doi.org/10.1007/s10295-004-0117-x.

[49] L. Perez, J. Vega, C. Chuay, A. Menendez, R. Ubieta, M. Montero, G. Padron, A. Silva, C. Santizo, V. Besada, ., Production and characterization of human gamma interferon from Escherichia coli, Appl. Microbiol Biotechnol 33 (1990) pp. 429-434.

[50] S.T. Vaiphei, G. Pandey, K.J. Mukherjee, Kinetic studies of recombinant human interferon-gamma expression in continuous cultures of E. coli, J Ind Microbiol Biotechnol 36 (2009) pp. 1453-1458. https://doi.org/10.1007/s10295-009-0632-x.

[51] J.G. Thomas and F. Baneyx, Roles of the Escherichia coli small heat shock proteins IbpA and IbpB in thermal stress management: comparison with ClpA, ClpB, and HtpG In vivo, J Bacteriol 180 (1998) pp. 5165-5172.

[52] C. Labarre, C. Divies, J. Guzzo, Genetic organization of the mle locus and identification of a mleR-like gene from Leuconostoc oenos, Appl. Environ. Microbiol 62 (1996) pp. 4493-4498.

[53] D. Piovesan, F. Tabaro, I. Micetic, M. Necci, F. Quaglia, C.J. Oldfield, M.C. Aspromonte, N.E. Davey, R. Davidovic, Z. Dosztanyi, A. Elofsson, A. Gasparini, A. Hatos, A.V. Kajava, L. Kalmar, E. Leonardi, T. Lazar, S. Macedo-Ribeiro, M. Macossay-Castillo, A. Meszaros, G. Minervini, N. Murvai, J. Pujols, D.B. Roche, E. Salladini, E. Schad, A. Schramm, B. Szabo, A. Tantos, F. Tonello, K.D. Tsirigos, N. Veljkovic, S. Ventura, W. Vranken, P. Warholm, V.N. Uversky, A.K. Dunker, S. Longhi, P. Tompa, S.C. Tosatto, DisProt 7.0: a major update of the database of disordered proteins, Nucleic Acids Res 45 (2017) p.D219-D227. https://doi.org/10.1093/nar/gkw1056.

[54] O. Conchillo-Sole, N.S. de Groot, F.X. Aviles, J. Vendrell, X. Daura, S. Ventura, AGGRESCAN: a server for the prediction and evaluation of "hot spots" of aggregation in polypeptides, BMC. Bioinformatics. 8 (2007) p.65. https://doi.org/10.1186/1471-2105-8-65.

[55] B. Zhou, L. Xing, W. Wu, X.E. Zhang, Z. Lin, Small surfactant-like peptides can drive soluble proteins into active aggregates, Microb Cell Fact 11 (2012) p.10. https://doi.org/10.1186/1475-2859-11-10.

[56] O. Cano-Garrido, F.L. Rueda, L. Sanchez-Garcia, L. Ruiz-Avila, R. Bosser, A. Villaverde, E. Garcia-Fruitos, Expanding the recombinant protein quality in *Lactococcus lactis*, Microb Cell Fact 13 (2014) p.167. https://doi.org/10.1186/s12934-014-0167-3.

[57] K. Spekker, M. Czesla, V. Ince, K. Heseler, S.K. Schmidt, G. Schares, W. Daubener, Indoleamine 2,3-dioxygenase is involved in defense against Neospora caninum in human and bovine cells, Infect. Immun. 77 (2009) pp. 4496-4501. https://doi.org/10.1128/IAI.00310-09.

[58] J.R. Lakowicz, J. Kusba, W. Wiczk, I. Gryczynski, H. Szmacinski, M.L. Johnson, Resolution of the conformational distribution and dynamics of a flexible molecule using frequency-domain fluorometry, Biophys. Chem 39 (1991) pp. 79-84.

[59] Y.C. Pan, A.S. Stern, P.C. Familletti, F.R. Khan, R. Chizzonite, Structural characterization of human interferon gamma. Heterogeneity of the carboxyl terminus, Eur. J Biochem 166 (1987) pp. 145-149.

[60] M. Kumar, M. Singh, S.B. Singh, Optimization of conditions for expression of recombinant interferon-gamma in E.coli, Mol Biol Rep. 41 (2014) pp. 6537-6543. https://doi.org/10.1007/s11033-014-3537-3.

[61] H. Billman-Jacobe, A.L. Hodgson, M. Lightowlers, P.R. Wood, A.J. Radford, Expression of ovine gamma interferon in Escherichia coli and Corynebacterium glutamicum, Appl. Environ. Microbiol 60 (1994) pp. 1641-1645.

[62] G.Y. Li, Z.Z. Xiao, H.P. Lu, Y.Y. Li, X.H. Zhou, X. Tan, X.Y. Zhang, X.L. Xia, H.C. Sun, A simple method for recombinant protein purification using self-assembling peptide-tagged tobacco etch virus protease, Protein Expr. Purif. 128 (2016) pp. 86-92. https://doi.org/10.1016/j.pep.2016.08.013.

[63] S. Bhattacharjee, DLS and zeta potential - What they are and what they are not?, J Control Release 235 (2016) pp. 337-351. https://doi.org/10.1016/j.jconrel.2016.06.017.

[64] A. Meager, Biological assays for interferons, J Immunol. Methods 261 (2002) pp. 21-36.

[65] M. Boyanova, R. Tsanev, I. Ivanov, A modified kynurenine bioassay for quantitative determination of human interferon-gamma, Anal. Biochem 308 (2002) pp. 178-181.

[66] A.K. Hess, P. Saffert, K. Liebeton, Z. Ignatova, Optimization of translation profiles enhances protein expression and solubility, PLoS One 10 (2015) p.e0127039. https://doi.org/10.1371/journal.pone.0127039.

[67] M. Boumaiza, A. Colarusso, E. Parrilli, E. Garcia-Fruitos, A. Casillo, A. Aris, M.M. Corsaro, D. Picone, S. Leone, M.L. Tutino, Getting value from the waste: recombinant production of a sweet protein by Lactococcus lactis grown on cheese whey, Microb Cell Fact 17 (2018) p.126. https://doi.org/10.1186/s12934-018-0974-z.

[68] G. Marini, M.D. Luchese, A.P. Argondizzo, A.C. de Goes, R. Galler, T.L. Alves, M.A. Medeiros, A.L. Larentis, Experimental design approach in recombinant protein expression: determining medium composition and induction conditions for expression of pneumolysin from Streptococcus pneumoniae in Escherichia coli and preliminary purification process, BMC. Biotechnol 14 (2014) p.1. https://doi.org/10.1186/1472-6750-14-1.

[69] E. Garcia-Fruitos, A. Aris, A. Villaverde, Localization of functional polypeptides in bacterial inclusion bodies, Appl. Environ. Microbiol 73 (2007) pp. 289-294. https://doi.org/10.1128/AEM.01952-06.

[70] A.K. Upadhyay, A. Murmu, A. Singh, A.K. Panda, Kinetics of inclusion body formation and its correlation with the characteristics of protein aggregates in Escherichia coli, PLoS One 7 (2012) p.e33951. 10.1371/journal.pone.0033951 [doi];PONE-D-11-18189 [pii].

[71] T. Hunig, The storm has cleared: lessons from the CD28 superagonist TGN1412 trial, Nat Rev. Immunol. 12 (2012) pp. 317-318. https://doi.org/10.1038/nri3192.

[72] G. Suntharalingam, M.R. Perry, S. Ward, S.J. Brett, A. Castello-Cortes, M.D. Brunner, N. Panoskaltsis, Cytokine storm in a phase 1 trial of the anti-CD28 monoclonal antibody TGN1412, N. Engl. J Med 355 (2006) pp. 1018-1028. https://doi.org/10.1056/NEJMoa063842.

[73] T.M. Li, J.W. Hook, III, H.G. Drickamer, G. Weber, Plurality of pressure-denatured forms in chymotrypsinogen and lysozyme, Biochemistry 15 (1976) pp. 5571-5580.

[74] R. Mohana-Borges, J.L. Silva, J. Ruiz-Sanz, G. de Prat-Gay, Folding of a pressure-denatured model protein, Proc Natl Acad Sci U S A 96 (1999) pp. 7888-7893.

[75] K. Ruan and G. Weber, Hysteresis and conformational drift of pressure-dissociated glyceraldehydephosphate dehydrogenase, Biochemistry 28 (1989) pp. 2144-2153.

[76] J.M. Sanchez, V. Nolan, M.A. Perillo, beta-galactosidase at the membrane-water interface: a case of an active enzyme with non-native conformation, Colloids Surf.

B Biointerfaces. 108 (2013) pp. 1-7.
https://doi.org/10.1016/j.colsurfb.2013.02.019.

[77] M. Randal and A.A. Kossiakoff, The 2.0 A structure of bovine interferon-gamma; assessment of the structural differences between species, Acta Crystallogr. D. Biol Crystallogr. 56 (2000) pp. 14-24.

[78] D.J. Thiel, M.H. le Du, R.L. Walter, A. D'Arcy, C. Chene, M. Fountoulakis, G. Garotta, F.K. Winkler, S.E. Ealick, Observation of an unexpected third receptor molecule in the crystal structure of human interferon-gamma receptor complex, Structure 8 (2000) pp. 927-936.

[79] S.S. Flores, V. Nolan, M.A. Perillo, J.M. Sanchez, Superactive beta-galactosidase inclusion bodies, Colloids Surf. B Biointerfaces. 173 (2019) pp. 769-775. https://doi.org/10.1016/j.colsurfb.2018.10.049.

[80] M. Martinez-Alonso, E. Garcia-Fruitos, A. Villaverde, Yield, solubility and conformational quality of soluble proteins are not simultaneously favored in recombinant Escherichia coli, Biotechnol Bioeng. 101 (2008) pp. 1353-1358. https://doi.org/10.1002/bit.21996.

[81] S. Ghobadi, M.R. Ashrafi-Kooshk, H. Mahdiuni, R. Khodarahmi, Enhancement of intrinsic fluorescence of human carbonic anhydrase II upon topiramate binding: Some evidence for drug-induced molecular contraction of the protein, Int J Biol Macromol. 108 (2018) pp. 240-249. https://doi.org/10.1016/j.ijbiomac.2017.12.011.

[82] L. Wang, Q. Dong, Q. Zhu, N. Tang, S. Jia, C. Xi, H. Zhao, S. Han, Y. Wang, Conformational Characteristics of Rice Hexokinase OsHXK7 as a Moonlighting Protein involved in Sugar Signalling and Metabolism, Protein J 36 (2017) pp. 249-256. https://doi.org/10.1007/s10930-017-9718-x.

Name	UNIPROT	HS region	HS size	Sequence	HSA	NHSA	a^4vAHS	Ref
CYOB	P0ABI8	591-629	39	AGIVIAAFSTIFGFAMIWHI WWLAIVGFAGMIITWIVKS	30.696	0.787	0.767	This study
HALRU	Q9BP37	1-17	17	MTYMCSILICLVLILCA	15.842	0.932	0.904	This study
L6K2	NA	1-6	6	LLLLLLKK	6.211	1.035	0.949	[55]

964 **Table 1** Selection of APPs from predictions of "hot spots (HS)" of aggregation in
965 polypeptides by AGGRESCAN [54]. CYOB: Cytochrome bo_3 ubiquinol oxidase subunit 1
966 from *E. coli*, HALRU: Aragonite protein AP7. NA: Not applicable. HS: hot spot. HSA: hot
967 spot area. NHSA: normalized HSA. a^4vAHS: average aggregation-propensity in each HS.

968

969

		Soluble rBoIFN-γ	rBoIFN-γ NPs		Soluble rBoIFN-γ from NPs
		CSM (nm)			
		Soluble	Protein NPs	NP core	Resolubilized
1	**rBoINF-γ_Std**	356.5			
2	**rBoIFN-γ_ *E. coli***	358.1			
3	**rBoIFN-γ_ *L. lactis***	357.4			
4	**rBoIFN-γ_*L. lactis***		**352.4**	353.6	**354.2**
5	**rBoIFN-γ_L6K2_*L. lactis***		**352.7**	353.6	**351.7**
6	**rBoIFN-γ_CYOB_*L. lactis***		353.1	353.1	354
7	**rBoIFNγ_HALRU_*L. lactis***		354.2	354.2	352

970

971 **Table 2** Center of spectral mass (CSM) of IFN-γ protein preparations in soluble formats or

972 in protein NPs analyzed before and after the resolubilization protocol.